Scattering by a Metallic Sphere Coated with Chiral Metamaterials

Mao Y. Wang[1], Nan Yang[1], Si C. Ye[1], Hai L. Li[1], Jun Xu[1], Cui L. Zhong[2], and Hu Zheng[1]

[1] School of Physical Electronics
University of Electronic Science and Technology of China, Cheng du, 610054, P.R. China
wmybrimlhl@163.com, yangnan1205@163.com, yesichao@gmail.com, hailong703@163.com,
xujun@uestc.edu.cn, huberyzheng@gmail.com.

[2] Centre of Integrated Electronics
Shenzhen Institutes of Advanced Technology, Chinese Academy of Sciences, Shenzhen, 518055, China
zhongcuilin@hotmail.com

Abstract ─ Co-polarized and cross-polarized electromagnetic scattering of a metallic sphere coated with chiral metamaterials (CMMs) are simulated with Mie series solution. Firstly, based on Bohren's decomposition technique, electromagnetic fields inside and outside of the sphere are expanded in spherical harmonics vector function. Then, the expanded coefficients are obtained in a suitable form for computation by applying the boundary conditions on the interfaces of all regions. The validity of Mie series solution is shown by computing backward scattering for a ferrite-coated metallic sphere. The effects to bistatic, forward and backward scattering caused by incident wave frequency, media parameters of a metallic sphere coated with CMMs are investigated in details.

Index Terms ─ Chiral, metamaterials, metallic, Mie series, and scattering.

I. INTRODUCTION

Recently, chiral metamaterials (CMMs) [1-6], which are artificial materials with large optical activity and circular dichroism have been proposed and made for polarization control applications at microwave and optical frequencies. CMMs lack any planes of mirror symmetry and possess strong ability to rotate the plane of polarization of electromagnetic waves. Due to geometric asymmetry, the cross-coupling between the electric and magnetic fields exists at the resonance. The chirality parameter β is used to describe the strength of the cross-coupling effect. Several geometric structures have been proposed to excite cross coupling, such as helices, Y structure, double-layered rosettes and crosswire structure and so on. Meanwhile negative refraction can be achieved by a chiral route. Due to the potential applications ranging from cloaking devices, sub-wavelength optical waveguides, to circular polarizer etc., interest in the study of CMMs has been growing both theoretically and experimentally. Analytical and numerical methods have been used to investigate wave propagation in chiral media [2-6] or metamaterials [7-9] such as Mie series solution, invariant embedding method, finite-difference time-domain method [10], and method of moments, etc. For three-dimensional structures, analytical Mie series solution [11-19] is more efficient and accurate than the others.

This paper is organized as follows: according to Bohren's decomposition technique, Mie series solution for a metallic sphere coated with chiral metamaterials is firstly deduced by applying electromagnetic fields expanded in spherical harmonics vector function inside and outside of the CMMs-coated metallic sphere to boundary conditions. Meanwhile, how to overcome the numerical instability of the Bessel function in the Mie series formula is presented. In section 3, co-polarized and cross-polarized bistatic forward and backward scattering of a metallic sphere coated with chiral metamaterials are calculated with Mie series solution to study its application in the cloak. Finally, conclusions are given.

II. THEORY

Figure 1 presents the geometry of the electromagnetic wave incident on a coated sphere with inner radius b and outer radius a [13, 16]. The time harmonic dependence $e^{(-i\omega t)}$ is assumed for all fields. The incident electromagnetic wave can be expanded in the vector spherical harmonics functions as,

$$\boldsymbol{E}^{inc} = \sum_{n=1}^{\infty} E_n \left[\boldsymbol{M}_{o1n}^{(1)}(k_0) - i\boldsymbol{N}_{e1n}^{(1)}(k_0) \right]$$

$$\boldsymbol{H}^{inc} = \frac{-k_3}{\omega\mu_3} \sum_{n=1}^{\infty} E_n \left[\boldsymbol{M}_{e1n}^{(1)}(k_0) + i\boldsymbol{N}_{o1n}^{(1)}(k_0) \right], \quad (1)$$

where $E_n = i^n E_0 (2n+1)/[n(n+1)]$. The notations $o1n$ and $e1n$ mean the summation form of both, the even and odd modes, respectively.
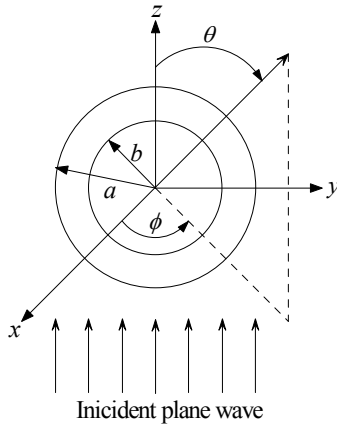
Fig. 1. A plane wave is incident on a metallic sphere coated with chiral metamaterials.

According to the Bohren's decomposition technique [13], the eigenfunction expansion in asymmetry chiral metamaterials can be written as a superposition of a left-handed and right-handed circularly polarized wave functions $\boldsymbol{v}_{o1n}^{(i)} = \boldsymbol{M}_{o1n}^{(i)} + \boldsymbol{N}_{o1n}^{(i)}$, $\boldsymbol{w}_{o1n}^{(i)} = \boldsymbol{M}_{o1n}^{(i)} - \boldsymbol{N}_{o1n}^{(i)}$, where i equals 1 or 3. The superscript "1" relates to the first type of spherical Bessel function and "3" relates the first kind of spherical Hankel function. The expansions of the scattered electromagnetic fields ($\boldsymbol{E}^s$, $\boldsymbol{H}^s$), and the electromagnetic fields ($\boldsymbol{E}^{chiral}$, $\boldsymbol{H}^{chiral}$) in the CMMs region $b < r < a$ are,

$$\boldsymbol{E}^s = \sum_{n=1}^{\infty} E_n \left[a_n^o \boldsymbol{M}_{o1n}^{(3)}(k_0) - ib_n^e \boldsymbol{N}_{e1n}^{(3)}(k_0) \right.$$
$$\left. + a_n^e \boldsymbol{M}_{e1n}^{(3)}(k_0) - ib_n^o \boldsymbol{N}_{o1n}^{(3)}(k_0) \right]$$

$$\boldsymbol{H}^s = -\frac{k_3}{\omega\mu_3} \sum_{n=1}^{\infty} E_n \left[b_n^e \boldsymbol{M}_{e1n}^{(3)}(k_0) + ia_n^o \boldsymbol{N}_{o1n}^{(3)}(k_0) \right.$$
$$\left. + b_n^o \boldsymbol{M}_{o1n}^{(3)}(k_0) + ia_n^e \boldsymbol{N}_{e1n}^{(3)}(k_0) \right],$$

$$\boldsymbol{E}^{chiral} = \sum_{n=1}^{\infty} E_n \left\{ \left[c_{1n}^o \boldsymbol{v}_{o1n}^{(1)}(k_L) + c_{2n}^o \boldsymbol{v}_{o1n}^{(3)}(k_L) \right. \right.$$
$$\left. + c_{1n}^e \boldsymbol{v}_{e1n}^{(1)}(k_L) + c_{2n}^e \boldsymbol{v}_{e1n}^{(3)}(k_L) \right]$$
$$- i\eta_c \left[d_{1n}^o \boldsymbol{w}_{o1n}^{(1)}(k_R) + d_{2n}^o \boldsymbol{w}_{o1n}^{(3)}(k_R) \right.$$
$$\left. \left. + d_{1n}^e \boldsymbol{w}_{e1n}^{(1)}(k_R) + d_{2n}^e \boldsymbol{w}_{e1n}^{(3)}(k_R) \right] \right\},$$

$$\boldsymbol{H}^{chiral} = \sum_{n=1}^{\infty} E_n \left\{ -i\left[c_{1n}^o \boldsymbol{v}_{o1n}^{(1)}(k_L) + c_{2n}^o \boldsymbol{v}_{o1n}^{(3)}(k_L) \right. \right.$$
$$\left. + c_{1n}^e \boldsymbol{v}_{e1n}^{(1)}(k_L) + c_{2n}^e \boldsymbol{v}_{e1n}^{(3)}(k_L) \right]/\eta_c \quad (2)$$
$$+ \left[d_{1n}^o \boldsymbol{w}_{o1n}^{(1)}(k_R) + d_{2n}^o \boldsymbol{w}_{o1n}^{(3)}(k_R) \right.$$
$$\left. \left. + d_{1n}^e \boldsymbol{w}_{e1n}^{(1)}(k_R) + d_{2n}^e \boldsymbol{w}_{e1n}^{(3)}(k_R) \right] \right\},$$

where $\eta_c = (\mu/\varepsilon)^{1/2}$, $k = \omega(\varepsilon_r \varepsilon_0 \mu_r \mu_0)^{1/2}$, $k_R = k/(1+\beta k)$, $k_L = k/(1-\beta k)$, ε_r, μ_r and β are the relative permittivity, relative permeability and chirality parameter of CMMs, respectively.

The unknown coefficients a_n^o, b_n^o, a_n^e, b_n^e of the scattered fields can be obtained by applying the boundary conditions of continuous tangential electric and magnetic fields at $r = a$ and the tangential electric field of the metallic boundary being vanished at $r = b$ [8]. In order to avoid computing Bessel functions with complex components that produce numerical instabilities, the coefficients of the scattered fields can be rearranged in a suitable form for computation as below,

$$a_n^o = \frac{-\psi_n(x)}{\xi_n(x)}$$

$$\cdot \frac{\left[\eta_c' P_{1n}^{(1)}(R) D_n(x) - P_{2n}^{(2)}(R) \right] \left[P_{2n}^{(1)}(L) F_n(x) - \eta_c' P_{1n}^{(2)}(L) \right]}{\left[\eta_c' P_{1n}^{(1)}(R) F_n(x) - P_{2n}^{(2)}(R) \right] \left[P_{2n}^{(1)}(L) F_n(x) - \eta_c' P_{1n}^{(2)}(L) \right]}$$
$$\frac{+\left[\eta_c' P_{1n}^{(1)}(L) D_n(x) - P_{2n}^{(2)}(L) \right] \left[P_{2n}^{(1)}(R) F_n(x) - \eta_c' P_{1n}^{(2)}(R) \right]}{+\left[\eta_c' P_{1n}^{(1)}(L) F_n(x) - P_{2n}^{(2)}(L) \right] \left[P_{2n}^{(1)}(R) F_n(x) - \eta_c' P_{1n}^{(2)}(R) \right]},$$

$$b_n^o = \frac{\left[P_{1n}^{(2)}(L)P_{2n}^{(1)}(R) - P_{1n}^{(2)}(R)P_{2n}^{(1)}(L) \right] \psi_n(x)}{\left[P_{1n}^{(1)}(L) \, P_{2n}^{(2)}(R) - P_{1n}^{(1)}(R)P_{2n}^{(2)}(L) \right] \xi_n(x)}$$

$$\cdot \frac{\begin{array}{l}\left[\eta_c' P_{1n}^{(1)}(R)D_n(x) - P_{2n}^{(2)}(R) \right]\left[-\eta_c' P_{1n}^{(1)}(L)F_n(x) + P_{2n}^{(2)}(L) \right] + \\ \left[\eta_c' P_{1n}^{(1)}(L)D_n(x) - P_{2n}^{(2)}(L) \right]\left[\eta_c' P_{1n}^{(1)}(R)F_n(x) - P_{2n}^{(2)}(R) \right]\end{array}}{\begin{array}{l}\left[\eta_c' P_{1n}^{(1)}(R)F_n(x) - P_{2n}^{(2)}(R) \right]\left[-\eta_c' P_{1n}^{(2)}(L) + P_{2n}^{(1)}(L)F_n(x) \right] + \\ \left[\eta_c' P_{1n}^{(1)}(L)F_n(x) - P_{2n}^{(2)}(L) \right]\left[-\eta_c' P_{1n}^{(2)}(R) + P_{2n}^{(1)}(R)F_n(x) \right]\end{array}},$$

$$a_n^e = -\frac{\left[P_{1n}^{(1)}(R)P_{2n}^{(2)}(L) - P_{1n}^{(1)}(L)P_{2n}^{(2)}(R) \right] \psi_n(x)}{\left[P_{1n}^{(2)}(R)P_{2n}^{(1)}(L) - P_{1n}^{(2)}(L)P_{2n}^{(1)}(R) \right] \xi_n(x)}$$

$$\cdot \frac{\begin{array}{l}\left[P_{2n}^{(1)}(R)D_n(x) - \eta_c' P_{1n}^{(2)}(R) \right]\left[P_{2n}^{(1)}(L)F_n(x) - \eta_c' P_{1n}^{(2)}(L) \right] + \\ \left[\eta_c' P_{1n}^{(2)}(L) - P_{2n}^{(1)}(L)D_n(x) \right]\left[P_{2n}^{(1)}(R)F_n(x) - \eta_c' P_{1n}^{(2)}(R) \right]\end{array}}{\begin{array}{l}\left[P_{2n}^{(2)}(L) - \eta_c' P_{1n}^{(1)}(L)F_n(x) \right]\left[P_{2n}^{(1)}(R)F_n(x) - \eta_c' P_{1n}^{(2)}(R) \right] + \\ \left[P_{2n}^{(2)}(R) - \eta_c' P_{1n}^{(1)}(R)F_n(x) \right]\left[P_{2n}^{(1)}(L)F_n(x) - \eta_c' P_{1n}^{(2)}(L) \right]\end{array}},$$

$$b_n^e = \frac{\psi_n(x)}{\xi_n(x)}$$

$$\cdot \frac{\begin{array}{l}\left[P_{2n}^{(1)}(R)D_n(x) - \eta_c' P_{1n}^{(2)}(R) \right]\left[\eta_c' P_{1n}^{(1)}(L)F_n(x) - P_{2n}^{(2)}(L) \right] \\ +\left[P_{2n}^{(1)}(L)D_n(x) - \eta_c' P_{1n}^{(2)}(L) \right]\left[\eta_c' P_{1n}^{(1)}(R)F_n(x) - P_{2n}^{(2)}(R) \right]\end{array}}{\begin{array}{l}\left[P_{2n}^{(1)}(R)F_n(x) - \eta_c' P_{1n}^{(2)}(R) \right]\left[\eta_c' P_{1n}^{(1)}(L)F_n(x) - P_{2n}^{(2)}(L) \right] \\ +\left[P_{2n}^{(1)}(L)F_n(x) - \eta_c' P_{1n}^{(2)}(L) \right]\left[\eta_c' P_{1n}^{(1)}(R)F_n(x) - P_{2n}^{(2)}(R) \right]\end{array}},$$

$$(3)$$

with

$$P_{2n}^{(1)}(R) = \frac{\psi_n(x_R^a)}{x_R^a} - Q_n(R)\frac{\xi_n(x_R^a)}{x_R^a} - G_n(R)\frac{\xi_n(x_L^a)}{x_L^a},$$

$$P_{2n}^{(2)}(R) = \frac{\psi_n'(x_R^a)}{x_R^a} - Q_n(R)\frac{\xi_n'(x_R^a)}{x_R^a} + G_n(R)\frac{\xi_n'(x_L^a)}{x_L^a},$$

$$P_{1n}^{(1)}(R) = \frac{\psi_n(x_R^a)}{x_R^a} - Q_n(R)\frac{\xi_n(x_R^a)}{x_R^a} + G_n(R)\frac{\xi_n(x_L^a)}{x_L^a},$$

$$P_{1n}^{(2)}(R) = \frac{\psi_n'(x_R^a)}{x_R^a} - Q_n(R)\frac{\xi_n'(x_R^a)}{x_R^a} - G_n(R)\frac{\xi_n'(x_L^a)}{x_L^a},$$

$$P_{2n}^{(1)}(L) = \frac{\psi_n(x_L^a)}{x_L^a} - Q_n(L)\frac{\xi_n(x_L^a)}{x_L^a} - G_n(L)\frac{\xi_n(x_R^a)}{x_R^a},$$

$$P_{2n}^{(2)}(L) = \frac{\psi_n'(x_L^a)}{x_L^a} - Q_n(L)\frac{\xi_n'(x_L^a)}{x_L^a} + G_n(L)\frac{\xi_n'(x_R^a)}{x_R^a},$$

$$P_{1n}^{(1)}(L) = \frac{\psi_n(x_L^a)}{x_L^a} - Q_n(L)\frac{\xi_n(x_L^a)}{x_L^a} + G_n(L)\frac{\xi_n(x_R^a)}{x_R^a},$$

$$P_{1n}^{(2)}(L) = \frac{\psi_n'(x_L^a)}{x_L^a} - Q_n(L)\frac{\xi_n'(x_L^a)}{x_L^a} - G_n(L)\frac{\xi_n'(x_R^a)}{x_R^a},$$

$$Q_n(R) = \frac{\left[F_n(x_L^b) - \dfrac{n}{x_R^b} \right]\psi_n(x_R^b) + \psi_{n-1}(x_R^b)}{\left[F_n(x_L^b) - \dfrac{n}{x_R^b} \right]\xi_n(x_R^b) + \xi_{n-1}(x_R^b)},$$

$$Q_n(L) = \frac{\left[F_n(x_R^b) - \dfrac{n}{x_L^b} \right]\psi_n(x_L^b) + \psi_{n-1}(x_L^b)}{\left[F_n(x_R^b) - \dfrac{n}{x_L^b} \right]\xi_n(x_L^b) + \xi_{n-1}(x_L^b)},$$

$$G_n(R) = \left(\frac{x_L^b}{x_R^b} \right)\frac{\left[F_n(x_R^b) + \dfrac{n}{x_R^b} \right]\psi_n(x_R^b) - \psi_{n-1}(x_R^b)}{\left[\dfrac{n}{x_L^b} - F_n(x_R^b) \right]\xi_n(x_L^b) - \xi_{n-1}(x_L^b)},$$

$$G_n(L) = \left(\frac{x_R^b}{x_L^b} \right)\frac{\left[F_n(x_L^b) + \dfrac{n}{x_L^b} \right]\psi_n(x_L^b) - \psi_{n-1}(x_L^b)}{\left[\dfrac{n}{x_R^b} - F_n(x_L^b) \right]\xi_n(x_R^b) - \xi_{n-1}(x_R^b)},$$

$$x_L^a = k_L a, \, x_R^a = k_R a,$$

$$x_L^b = k_L b, \, x_R^b = k_R b,$$

$$\psi_n(x) = xj_n(x),$$

$$\xi_n(x) = xh_n^{(1)}(x),$$

$$\eta_c' = \eta_c / \sqrt{\mu_0 / \varepsilon_0},$$

$$D_n(x) = \psi_n'(x) / \psi_n(x),$$

$$F_n(x) = \xi_n'(x) / \xi_n(x), \qquad (4)$$

$$D_{n-1}(\sigma) = \frac{\psi_{n-1}'(\sigma)}{\psi_{n-1}(\sigma)} = \frac{n}{\sigma} - \frac{1}{D_n + n/\sigma}, \qquad (5)$$

$$F_n(\sigma) = \xi_n'(\sigma) / \xi_n(\sigma) = \xi_{n-1}(\sigma) / \xi_n(\sigma) - n / \sigma.$$

D_n can be stably computed by downward recursion, while F_n can be stably computed by forward recursion [8]. With the assumption that the plane of interest is defined by $\phi = 0^\circ$, the co-polarized bistatic radar cross section (RCS) $\sigma_{\theta\theta}$, $\sigma_{\phi\phi}$, and the cross-polarized bistatic RCS $\sigma_{\phi\theta}$ of a metallic sphere coated with CMMs can be obtained as,

$$\sigma_{\theta\theta} = \frac{\lambda_0^2}{\pi}\left| \sum_{n=1}^{\infty}\left[\frac{2n+1}{n(n+1)}(b_n^e\tau_n + a_n^o\pi_n) \right] \right|^2$$

$$\sigma_{\phi\phi} = \frac{\lambda_0^2}{\pi}\left| \sum_{n=1}^{\infty}\left[\frac{2n+1}{n(n+1)}(b_n^e\pi_n + a_n^o\tau_n) \right] \right|^2,$$

$$\sigma_{\phi\theta} = \frac{\lambda_0^2}{\pi}\left| \sum_{n=1}^{\infty}\left[\frac{2n+1}{n(n+1)}(b_n^o\pi_n - a_n^e\tau_n) \right] \right|^2, \qquad (6)$$

with

$$\pi_n = P_n^1(\cos\theta)/\sin\theta,$$

$$\tau_n = -\sin\theta P_n^{1\prime}(\cos\theta), \qquad (7)$$

where P_n^1 is the Legendre function.

III. NUMERICAL RESULTS

In this section, numerical results about scattering by a metallic sphere coated with CMMs are illustrated. Bistatic, forward and backward radar cross sections, which are generally dependent upon various parameters characterizing the geometry, material properties, and incident fields, are discussed below.

A. Example verification

The validity of Mie series solution in the paper is verified with the results in reference [11]. Figure 2 presents the backward scattering versus the radius for a 0.01 m depth metallic sphere coated with different kinds of media. The wavelength of the incident wave λ_0 is chosen to be 0.01 m, the thickness $t = a–b$ of the media coating layer is $0.05\lambda_0$. The curve consisting of crosses represent backward scattering of a bald metallic sphere. The solid line, dash line, dotted line, and circular curve represents the backward scattering of a metallic sphere coated with lossless ferrite ($\varepsilon_r = 2.5$, $\mu_r = 1.6$), lossy ferrite ($\varepsilon_r = 2.5+i1.25$, $\mu_r = 1.6+i0.8$), lossy metamaterials ($\varepsilon_r = -2.5+i1.25$, $\mu_r = -1.6+i0.8$), and lossy chiral media ($\varepsilon_r = 2.5+i1.25$, $\mu_r = 1.6+i0.8$, $\beta = 9\times10^{-4}$), respectively.

In Fig. 2, the dash line has an excellent agreement with the asterisk for the backward scattering data in reference [11]. Lossy ferrite, metamaterials, and chiral media can make backward scattering decrease at relatively wide electrical size. The backward RCS of a metallic sphere coated with lossy metamaterials and lossy chiral media vary relatively slower as the radius increases. Though the skin depth of each kinds of media coating and the incident wave frequency are numerically identical, it may be noted in Fig. 2 that the backward scattering of a metallic sphere coated with lossy chiral media is significantly smaller than the other media coating.
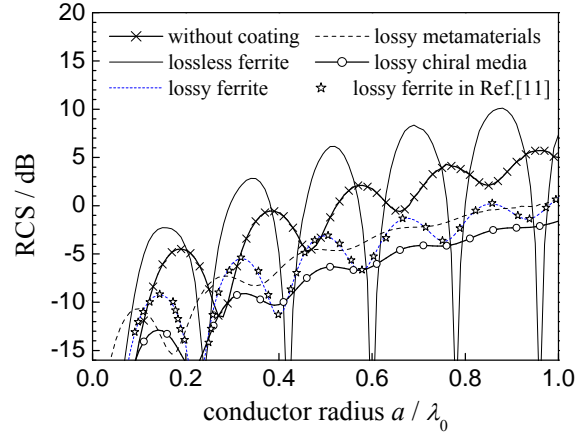
Fig. 2. Backward scattering versus radius for a metallic sphere with ferrite, metamaterials, or chiral media coating.

B. Bistatic RCS

Figure 3 presents the bistatic co-polarized E-plane with a bistatic RCS of $\sigma_{\theta\theta}$ and a co-polarized H-plane with a bistatic RCS of $\sigma_{\phi\phi}$. In addition to the cross-polarized RCS patterns for a metallic sphere coated with CMMs, having $\varepsilon_r = -4.0$, $\mu_r = -1.0$, and $\beta = 0.006$. The radius b of the metallic sphere is 0.382 cm and the outer radius a of the chiral metamaterials shown in Fig. 1 is 1.528 cm [20]. The arrow indicates the direction of the plane wave incidence. The Mie series solution spans incident wave frequencies 3 GHz, 9.375 GHz, and 18 GHz. For the sake of brevity in the paper, only half of the bistatic scattering patterns are shown.

As shown in Fig. 3, the co-polarized and cross-polarized bistatic radar cross sections are relatively smaller at most angles as the 3GHz electromagnetic wave incident. When the incident wave frequency increase, both co-polarized forward scattering and resonant characteristic of a metallic sphere coated with CMMs obviously increase.

(a)

(b)

(c)
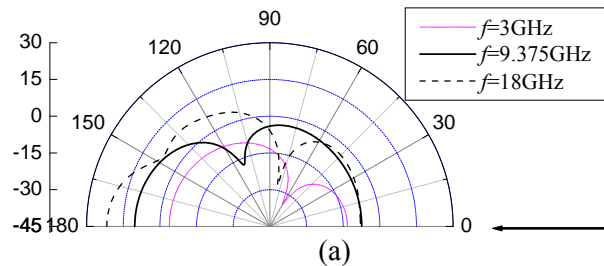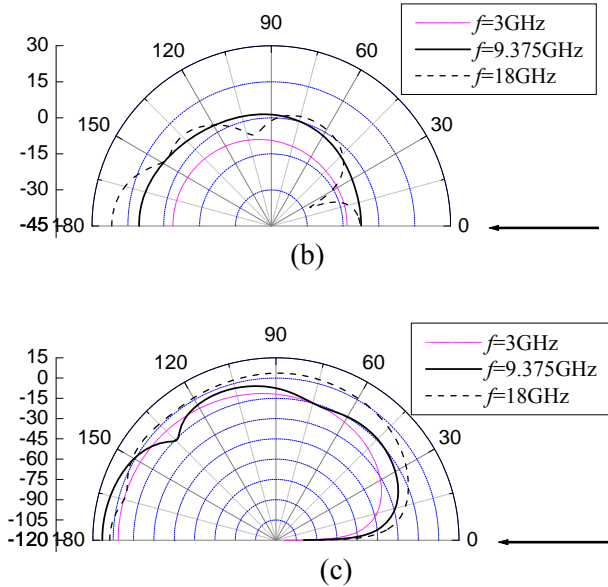
Fig. 3. Bistatic RCS patterns for a metallic sphere coated with CMMs for the (a) co-polarized E-plane, (b) co-polarized H-plane, and (c) cross-polarized RCS.

C. Forward RCS

Figure 4 compares the forward scattering response of a 10 cm radius metallic sphere and a 10 cm radius metallic sphere coated with 1 cm thickness CMMs as a function of electrical size. The cross-polarized scattering of a bald metallic is zero. The circular curve, curve consisting of crosses, solid line, and dotted line represent the imposed condition without the coating layer, coated with lossy chiral metamaterials case I ($\varepsilon_r = \mu_r = -1$, $\beta = 0.001$), case II ($\varepsilon_r = \mu_r = -2$, $\beta = 0.001$), case III ($\varepsilon_r = \mu_r = -0.5$, $\beta = 0.001$), respectively. As can be seen from Fig. 4, a metallic sphere coated with CMMs cast a larger shadow than a metallic sphere. Though the introduction of chiral parameter destroy the impedance match characteristic of matched metamaterials with $\varepsilon_r = \mu_r$, $\beta = 0$, the co-polarized, and cross-polarized forward scattering of a metallic sphere coated with lossy CMMs case I has a well-defined trend, in a manner consistent with the forward scattering of a metallic sphere. Compared to the co-polarized, the cross-polarized forward scattering is relatively smaller. A metallic sphere coated with chiral metamaterials case III ($\varepsilon_r = \mu_r = -0.5$, $\beta = 0.001$) has relatively more surface modes, due to the resonant effect related to the Mie scattering coefficients.

(a)

(b)
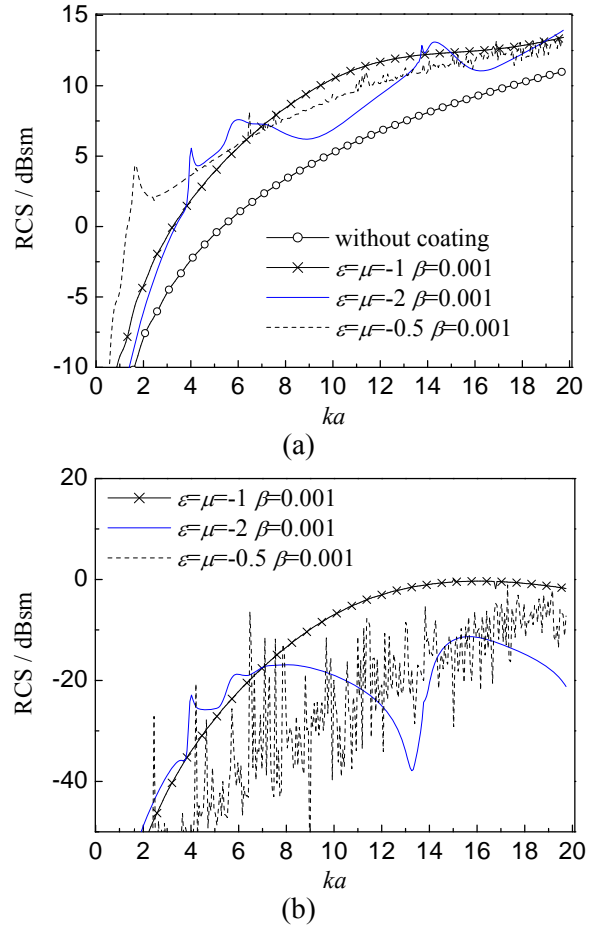
Fig. 4. Forward scattering from a 10 cm radius metallic sphere coated with CMMs for both the (a) co-polarized and the (b) cross-polarized.

D. Backward RCS

Figure 5 illustrates the co-polarized and cross-polarized backward scattering of a relatively large 10 cm radius metallic sphere coated with 1 cm thickness for different kinds of media. In Fig. 5 (a), the curve consisting of crosses and circular curve represent the co-polarized backward scattering of a bald metallic sphere and a metallic sphere coated with chiral metamaterials ($\varepsilon_r = -2.5$, $\mu_r = -1.6$, and $\beta = 0.005$). From 2.2 GHz to 2.7 GHz, the chiral metamaterials make the backward RCS of metallic sphere evidently decrease. One of the possible reasons is the negative refractive properties of the chiral metamaterials, which makes the refracted wave go back to the front surface of the metallic sphere and produce a shadowing effect on the back region. The other possible reason is the chirality parameter, which

induces the cross-polarized wave. The cross-polarized scattering in Fig. 5 (b) is nearly negligible as the value of chirality parameter β is relatively small.

(a)

(b)
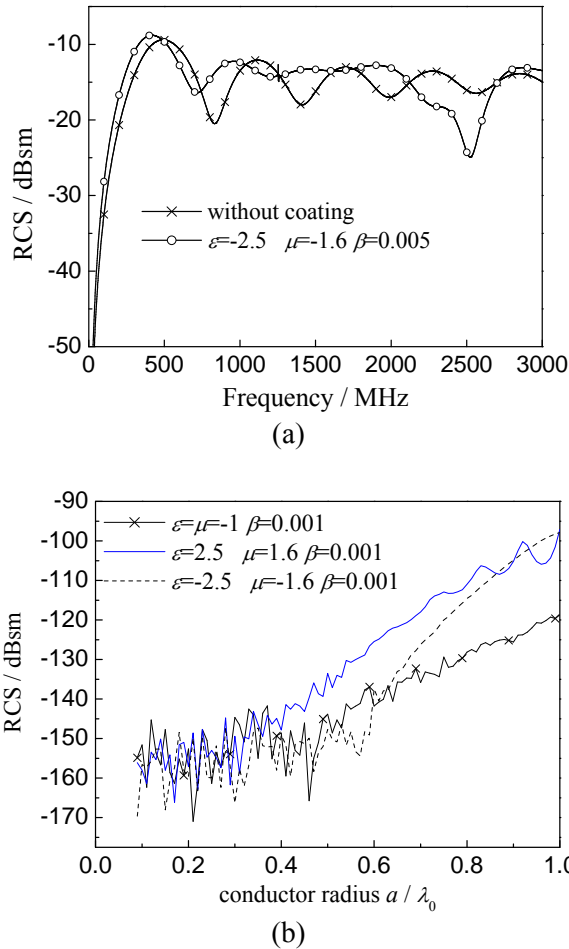
Fig. 5. Backward scattering response of a metallic sphere coated with different kinds of media for both (a) co-polarized and (b) cross-polarized.

IV. CONCLUSIONS

This paper presents Mie theory for electromagnetic scattering by a perfectly metallic sphere with a uniform coating of chiral metamaterials. How to overcome the numerical instability of the Bessel function in the series formula is given. Co-polarized and cross-polarized bistatic scattering patterns, forward and backward radar cross section of a metallic sphere coated with chiral metamaterials are illustrated. Numerical results show that the co-polarized forward scattering and the resonant surface modes of a metallic sphere coated with CMMs increase with increasing the frequency of the incident wave. Compared to the co-polarized scattering, the cross-polarized scattering are relatively smaller. Due to the negative refractive property and giant optical activity, CMMs can make the echo of a metallic sphere decrease to a certain degree.

REFERENCES

[1] J. B. Pendry, "A chiral route to negative refraction," *Science*, vol. 306, no. 5700, pp. 1353-1355, 2004.

[2] E. K. Yung and B. J. Hu, "Scattering by conducting sphere coated with chiral media," *Microw. Opt. Techn. Let.*, vol. 35, no. 4, pp. 288-293, 2002.

[3] S. Tretyakov, I. Nefedov, A. Sihvola, S. Maslovski, and C. Simovski, "Waves and energy in chiral nihility," *J. Electro. Wave*, vol. 17, no. 5, pp. 695-706, 2003.

[4] D. V. Guzatov and V. V. Klimov, "Chiral particles in a circularly polarised light field: new effects and applications," *Quantum Electronics*, vol. 41, no. 6, pp. 526-533, 2011.

[5] A. M. Attiya, "Coupled mode analysis of two-dimensional chiral grating," *Appl. Comp. Electro. Society*, vol. 26, no. 4, pp. 303-311, 2011.

[6] S. T. Imeci, F. Altunkilic, J. R. Mautz, and E. Arvas, "Transmission through an arbitrarily shaped aperture in a conducting plane separating air and a chiral medium," *Appl. Comp. Electro. Society*, vol. 25, no. 7, pp. 587-599, 2010.

[7] J. M. Taboada, M. G. Araújo, J. Rivero, L. Landesa, and F. Obelleiro, "Surface integral equation solvers for large-scale conductors, metamaterials and plasmonic nanostructures," *Appl. Comp. Electro. Society*, vol. 27, no. 2, pp. 189-197, 2012.

[8] L. Gaoa and Y. Y. Huang, "Extinction properties of a coated sphere containing a left-handed material," *Opt. Commun.*, vol. 239, no. 1-3, pp. 25-31, 2004.

[9] M. I. Aksun, A. Alparslan, E. P. Karabulut, E. Irci, and V. B. Ertürk, "Determining the effective constitutive parameters of finite periodic structures: photonic crystals and metamaterials," *IEEE Trans. Microwave Theory and Tech.*, vol. 56, no. 6, pp. 1423-1434, 2010.

[10] J. A. Pereda, A. Grande, O. González, and Á. Vegas,

"FDTD modeling of chiral media by using the mobius transformation technique," *IEEE Antennas and Wireless Propagation Letters*, vol. 5, no. 3, pp. 327-330, 2006.

[11] J. H. Richmond, "Scattering by a ferrite-coated conducting sphere," *IEEE Trans. Antennas Propagat.*, vol. 35, no. 1, pp. 73-79, 1987.

[12] D. J. Ross and R. Sigel, "Mie scattering by soft core-shell particles and its applications to ellipsometric light scattering," *Phys. Rev. E*, vol. 85, no. 5, pp. 1-13, 2012.

[13] C. F. Bohren and D. R. Huffman, *Absorption and scattering of light by small particles*, Wiley, New York, 1983.

[14] Z. S. Wu and Y. P. Wang, "Electromagnetic scattering for multilayered sphere: recursive algorithms," *Radio Sci.*, vol. 26, no. 6, pp. 1393-1401, 1991.

[15] Z. W. Zhao, Z. S. Wu, and Q. Z. Xue, "An algorithm for electromagnetic scattering of large absorptive homogeneous sphere," *Chinese Journal of Radio Science*, vol. 14, no. 4, pp. 422-425, 1999.

[16] V. Demir, A. Elsherbeni, and D. Worasawate, "A graphical user interface (GUI) for plane wave scattering from a conducting, dielectric or a chiral Sphere," *IEEE Antenn. Propag. Mag.*, vol. 46, no. 5, pp. 94-99, 2004.

[17] Y. L. Geng and S. L. He, "Analytical solution for electromagnetic scattering from a sphere of uniaxial left-handed material," *J. Zhejiang Univ.-Sc. A*, vol. 17, no. 1, pp. 99-104, 2006.

[18] Z. W. Zhao, Z. S. Wu, and Q. Z. Xue, "An algorithm for electromagnetic scattering of large absorptive homogeneous sphere," *Chinese Journal of Radio Science*, vol. 14, no. 4, pp. 422-425, 1999.

[19] M. Y. Wang, C. W. Qiu, J. Xu, Y. L. Dong, H. Zheng, and H. L. Li, "MIE series for electromagnetic scattering of chiral metamaterials sphere," *Journal of Systems Engineering and Electronics*, vol. 22, no. 6, pp. 885-891, 2011.

[20] D. B. Ge and Y. B. Yan, "Finite-difference time-domain method for electromagnetic waves," *Xi'an University Press*, 2011.

Mao Yan Wang was born in Shandong, China, 1979. She is currently an Associate Professor with University of Electronic Science and Technology of China (UESTC). Her research interests include millimeter wave circuit and systems, computation electromagnetic and metamaterials.

Nan Yang was born in Shandong, China, 1990. She is currently working toward the Master degree in Radio Physics at UESTC. Her research interest is millimeter wave circuit and systems.

Si Chao Ye was born in Si chuan,China,1990. He is currently working toward the M.Sc. degree in Radio physics at UESTC. His research interest is millimeter wave systems.

Hai Long Li was born in Shandong, China, in 1979. He is currently an Associate Professor with UESTC. His research interests include dusty plasma and high-power microwave technique.

Jun Xu was born in 1963. He is currently a Professor with UESTC. His research interests include millimeter wave hybrid integrated technology, communication and radar RF technology.

Cui Lin Zhong was born in Hunan, China, 1975. His current research interests include microwaves, antenna techniques, and radio technology of wireless communication and radar.
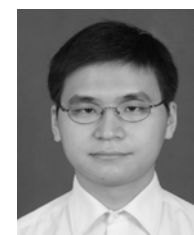
Hu Zheng was born in 1979. He is an Associate Professor with UESTC. His research interests include EM theory and microwave technology and computation electromagnetic etc.